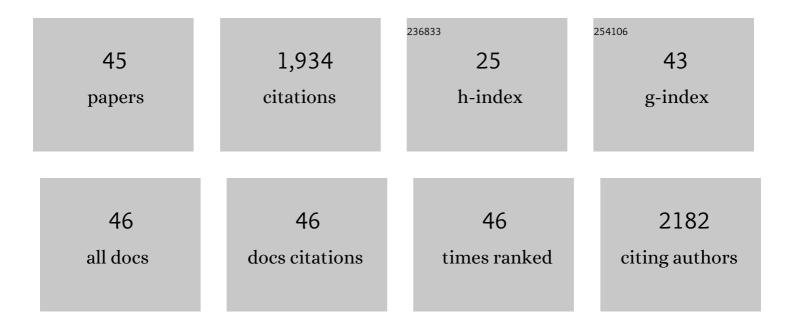
## Huan-Ping Jing

List of Publications by Year in descending order

Source: https://exaly.com/author-pdf/8741142/publications.pdf Version: 2024-02-01



#	Article	IF	CITATIONS
1	Enhanced visible light photo-Fenton-like degradation of tetracyclines by expanded perlite supported FeMo3Ox/g-C3N4 floating Z-scheme catalyst. Journal of Hazardous Materials, 2022, 424, 127387.	6.5	83
2	In-situ remediation of zinc contaminated soil using phosphorus recovery product: Hydroxyapatite/calcium silicate hydrate (HAP/C–S–H). Chemosphere, 2022, 286, 131664.	4.2	13
3	Simultaneous adsorption and oxidation of Sb(III) from water by the pH-sensitive superabsorbent polymer hydrogel incorporated with Fe-Mn binary oxides composite. Journal of Hazardous Materials, 2022, 423, 127013.	6.5	30
4	Activation of peroxymonosulfate by a floating oxygen vacancies - CuFe2O4 photocatalyst under visible light for efficient degradation of sulfamethazine. Science of the Total Environment, 2022, 824, 153630.	3.9	35
5	Effect of biofilm colonization on Pb(II) adsorption onto poly(butylene succinate) microplastic during its biodegradation. Science of the Total Environment, 2022, 833, 155251.	3.9	24
6	Remediation of artificially contaminated soil and groundwater with copper using hydroxyapatite/calcium silicate hydrate recovered from phosphorus-rich wastewater. Environmental Pollution, 2021, 272, 115978.	3.7	21
7	Visible-light-driven heterostructured g-C3N4/Bi-TiO2 floating photocatalyst with enhanced charge carrier separation for photocatalytic inactivation of Microcystis aeruginosa. Frontiers of Environmental Science and Engineering, 2021, 15, 1.	3.3	39
8	Hydrous manganese dioxide modified poly(sodium acrylate) hydrogel composite as a novel adsorbent for enhanced removal of tetracycline and lead from water. Chemosphere, 2021, 272, 129902.	4.2	27
9	Efficient elimination of the pollutants in eutrophicated water with carbon strengthened expanded graphite based photocatalysts: Unveiling the synergistic role of metal sites. Journal of Hazardous Materials, 2021, 416, 125729.	6.5	4
10	Enhanced removal of oxytetracycline antibiotics from water using manganese dioxide impregnated hydrogel composite: Adsorption behavior and oxidative degradation pathways. Chemosphere, 2021, 280, 130926.	4.2	38
11	Effects of coexistence of tetracycline, copper and microplastics on the fate of antibiotic resistance genes in manured soil. Science of the Total Environment, 2021, 790, 148087.	3.9	47
12	Application of graphene-based materials for removal of tetracyclines using adsorption and photocatalytic-degradation: A review. Journal of Environmental Management, 2020, 276, 111310.	3.8	130
13	Reduction and immobilization of Cr(VI) in aqueous solutions by blast furnace slag supported sulfidized nanoscale zerovalent iron. Science of the Total Environment, 2020, 743, 140722.	3.9	52
14	Struvite-supported biochar composite effectively lowers Cu bio-availability and the abundance of antibiotic-resistance genes in soil. Science of the Total Environment, 2020, 724, 138294.	3.9	27
15	Application of MgO-modified palygorskite for nutrient recovery from swine wastewater: effect of pH, ions, and organic acids. Environmental Science and Pollution Research, 2019, 26, 19729-19737.	2.7	11
16	Phosphate recovery from wastewater using calcium silicate hydrate (C-S-H): sonochemical synthesis and properties. Environmental Science: Water Research and Technology, 2019, 5, 131-139.	1.2	25
17	Effects of struvite-humic acid loaded biochar/bentonite composite amendment on Zn(II) and antibiotic resistance genes in manure-soil. Chemical Engineering Journal, 2019, 375, 122013.	6.6	41
18	In-situ active formation of carbides coated with NP TiO2 nanoparticles for efficient adsorption-photocatalytic inactivation of harmful algae in eutrophic water. Chemosphere, 2019, 228, 351-359.	4.2	31

Huan-Ping Jing

#	Article	IF	CITATIONS
19	Simultaneous recovery of phosphate, ammonium and humic acid from wastewater using a biochar supported Mg(OH) <sub>2</sub> /bentonite composite. Environmental Science: Water Research and Technology, 2019, 5, 931-943.	1.2	40
20	Sustainable utilization of a recovered struvite/diatomite compound for lead immobilization in contaminated soil: potential, mechanism, efficiency, and risk assessment. Environmental Science and Pollution Research, 2019, 26, 4890-4900.	2.7	7
21	Low-temperature preparation of a N-TiO2/macroporous resin photocatalyst to degrade organic pollutants. Environmental Chemistry Letters, 2019, 17, 1061-1066.	8.3	20
22	Comparison of palygorskite and struvite supported palygorskite derived from phosphate recovery in wastewater for in-situ immobilization of Cu, Pb and Cd in contaminated soil. Journal of Hazardous Materials, 2018, 346, 273-284.	6.5	34
23	Surface modified TiO2 floating photocatalyst with PDDA for efficient adsorption and photocatalytic inactivation of Microcystis aeruginosa. Water Research, 2018, 131, 320-333.	5.3	85
24	High zinc removal from water and soil using struvite-supported diatomite obtained by nitrogen and phosphate recovery from wastewater. Environmental Chemistry Letters, 2018, 16, 569-573.	8.3	8
25	Removal of cadmium (II) from aqueous solution: A comparative study of raw attapulgite clay and a reusable waste–struvite/attapulgite obtained from nutrient-rich wastewater. Journal of Hazardous Materials, 2017, 329, 66-76.	6.5	154
26	Syntheses and photocatalytic performances of four coordination complexes constructed from 1,10-phenanthroline and polycarboxylic acids. Transition Metal Chemistry, 2017, 42, 181-191.	0.7	4
27	Efficient visible light-driven in situ photocatalytic destruction of harmful alga by worm-like N,P co-doped TiO <sub>2</sub> /expanded graphite carbon layer (NPT-EGC) floating composites. Catalysis Science and Technology, 2017, 7, 2335-2346.	2.1	36
28	Synthesis and Characterization of MgO Modified Diatomite for Phosphorus Recovery in Eutrophic Water. Journal of Chemical & Engineering Data, 2017, 62, 226-235.	1.0	36
29	Enhanced sunlight photocatalytic activity and recycled Ag–N co-doped TiO2 supported by expanded graphite C/C composites for degradation of organic pollutants. Research on Chemical Intermediates, 2016, 42, 5541-5557.	1.3	11
30	Preparation, characterization, and photocatalytic activity evaluation of Fe–N-codoped TiO2/fly ash cenospheres floating photocatalyst. Environmental Science and Pollution Research, 2016, 23, 22793-22802.	2.7	21
31	Insight into visible light-driven photocatalytic degradation of diesel oil by doped TiO2-PS floating composites. Environmental Science and Pollution Research, 2016, 23, 18145-18153.	2.7	13
32	Recovery of nutrients from wastewater by a MgCl <sub>2</sub> modified zeolite and their reuse as an amendment for Cu and Pb immobilization in soil. RSC Advances, 2016, 6, 55809-55818.	1.7	15
33	Bioremediation of marine oil pollution by <i>Brevundimonas diminuta</i> : effect of salinity and nutrients. Desalination and Water Treatment, 2016, 57, 19768-19775.	1.0	32
34	Two Zinc Based Coordination Compounds Constructed from Two Azophenyl Ligands: Syntheses, Crystal Structure, and Photocatalytic Performance. Journal of Inorganic and Organometallic Polymers and Materials, 2016, 26, 276-284.	1.9	6
35	Three coordination compounds of cobalt with organic carboxylic acids and 1,10-phenanthroline as ligands: syntheses, structures and photocatalytic properties. Transition Metal Chemistry, 2015, 40, 573-584.	0.7	10
36	Enhanced visible light photocatalytic activity of a floating photocatalyst based on B–N-codoped TiO <sub>2</sub> grafted on expanded perlite. RSC Advances, 2015, 5, 41385-41392.	1.7	38

Huan-Ping Jing

#	Article	IF	CITATIONS
37	Floating photocatalysts based on loading Bi/N-doped TiO <sub>2</sub> on expanded graphite C/C (EGC) composites for the visible light degradation of diesel. RSC Advances, 2015, 5, 71922-71931.	1.7	33
38	Photocatalytic degradation of methylene blue in ZIF-8. RSC Advances, 2014, 4, 54454-54462.	1.7	401
39	Adsorption–photodegradation of humic acid in water by using ZnO coupled TiO2/bamboo charcoal under visible light irradiation. Journal of Hazardous Materials, 2013, 262, 16-24.	6.5	86
40	P-benzoquinone-mediated amperometric biosensor developed with Psychrobacter sp. for toxicity testing of heavy metals. Biosensors and Bioelectronics, 2013, 41, 557-562.	5.3	57
41	Cr(VI) removal from aqueous solution with bamboo charcoal chemically modified by iron and cobalt with the assistance of microwave. Journal of Environmental Sciences, 2013, 25, 1726-1735.	3.2	50
42	Reduction of hexavalent chromium with scrap iron in a fixed bed reactor. Frontiers of Environmental Science and Engineering, 2012, 6, 761-769.	3.3	6
43	Effect of Initial Nitrate Concentrations and Heavy Metals on Autohydrogenotrohic Denitrification. , 2009, , .		3
44	Biosorption of Direct Black 38 by dried anaerobic granular sludge. Frontiers of Environmental Science and Engineering in China, 2008, 2, 198-202.	0.8	2
45	Changes of Cu, Zn, and Ni chemical speciation in sewage sludge co-composted with sodium sulfide and lime. Journal of Environmental Sciences, 2008, 20, 156-160.	3.2	48